Chapter 17
Ion Traps

17.1 Introduction

Ion trap technology currently leads the way in the effort to gain complete control of quantum coherence in isolated systems. The seminal paper of Cirac and Zoller thrust the technology to the forefront of the quantum processing agenda in a seminal paper in 1995 [1]. Beginning over 30 years ago, experimentalists began trapping clouds of atomic ions in order to achieve higher spectroscopic resolution [2]. The heritage of this effort is the current ability to define time standards using ion trap clocks. Future developments will depend on the ability to make smaller trap arrays for quantum computing applications.

Ion trap technology also enables quantum limited measurements of the electronic and vibrational states of a single trapped ion using the method of cycling fluorescent transitions. This ability led to a complete reappraisal of how quantum mechanics of single systems, subject to continuous observation, should be interpreted [3] enabling an explicit physical demonstration of the concept of a quantum trajectory discussed in Chap. 6. It is possible to trap and cool a single ion close to its vibrational ground state [4], carefully prepare complex superpositions of energy eigenstates through optical excitation and then monitor the subsequent dynamics with extaordinary sensitivity.

17.2 Trapping and Cooling

Laplace's equation indicates that it is not possible to trap a charged particle in three dimensions with a static potential: there is always one unstable (untrapped) direction in an electrostatic potential. We must resort to time periodic potentials. In Fig. 17.1 we show a possible configuration of electrodes.

The time dependent potential can be written

$$V(x,y,z,t) = \frac{\bar{V}}{2}(k_x x^2 + k_y y^2 + k_z z^2) + \frac{1}{2}V\cos(\omega_{rf}t)(k'_x x^2 + k'_y y^2) \qquad (17.1)$$

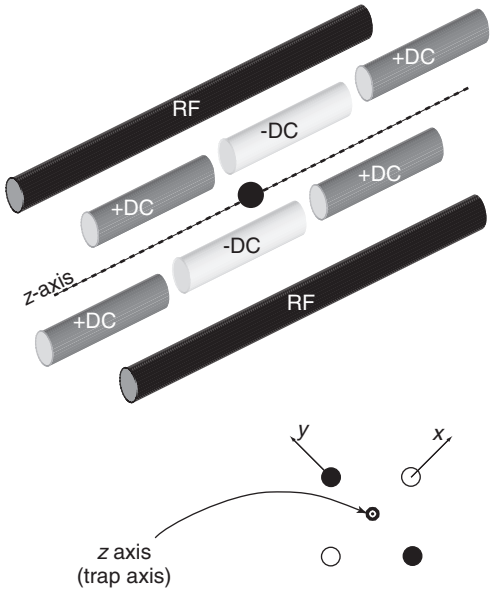

Fig. 17.1 A schematic representation of a linear radio frequency ion trap (after [5])

where ω_{rf} is the frequency of the time dependent potential. Laplace's equation implies, $k_x + k_y + k_z = 0$, $k'_x + k'_y = 0$. If we assume [5]

$$a_x = \frac{4Z|e|\bar{V}k_x}{m\omega_{rf}^2} << 1$$
$$q_x = \frac{2Z|e|Vk'_x}{m\omega_{rf}^2} << 1$$

then the motion in the x-direction is approximately harmonic, as is motion in the y-direction. Given isotropy in the $x-y$ plane, so that $k_x = k_y$, $k'_x = k'_y$ and the motion is harmonic with the secular frequency

$$\nu = \left(a_x + q_x^2/2\right)^{1/2} \omega_{rf}/2 \tag{17.2}$$

A small amplitude oscillatory motion at frequency ω_{rf} is superimposed on the secular motion, called the micromotion, which we neglect. In an experiment with $^9Be^+$, the axial frequency was about 3 MHz while the transverse frequency was about 8 MHz. The static potential due to end caps gives harmonic confinement along the trap axis (z-direction). If this is kept weak, multiple ions can be trapped in a line along the z-direction. Typically the transverse frequencies are three to four times more than the axial.

The centre-of-mass quantum dynamics of the ion is determined by the eigenstates of the Hamiltonian

$$H = \hbar\nu a_z^\dagger a_z + \hbar\nu_t (a_x^\dagger a_x + a_y^\dagger a_y) \tag{17.3}$$

The motion is thus separable into axial and transverse motion and, to be specific, we now concentrate on the axial motion alone. As we neglect the transverse motion, we will drop the subscript on $a_z, a_z^\dagger$.

The availability of lasers at appropriate atomic transition frequencies determine which ions can be successfully trapped and cooled. The Wineland group at NIST Colorado uses $^9Be^+$ while the Blatt group in Innsbruck uses $^{40}Ca^+$. After trapping it is necessary to remove vibrational energy from the ion, that is to say, it must be cooled. The initial temperature is of the order of 10^4 K. The first stage of cooling is based on Doppler cooling and is very efficient, the second stage is based on resolved sideband cooling (see below).

The extraordinary degree of control over quantum coherence that can be achieved in an ion trap is due to a number of reasons. Firstly, it is possible to coherently couple the vibrational motion and the internal electronic state using an external laser. Secondly, resolved sideband cooling enables the vibrational motion to be prepared in its ground state with probability approaching unity. External lasers induce Raman transitions between the ground and excited internal electronic state in which one phonon of vibrational energy is absorbed per excitation cycle. Finally, the internal electronic state of a single trapped ion can be determined with efficiency approaching unity by the method of fluorescence shelving enables.

We will assume that external lasers drive a two level transition from the ground state $|g\rangle$ to the excited state $|e\rangle$. This could be a direct dipole transition, but for quantum computing it typically involves a Raman two-photon transition connecting the ground state to an excited meta-stable state. In either case the Hamiltonian describing the system is (see 10.1),

$$H = \hbar\nu a^\dagger a + \hbar\omega_A \sigma_z + \frac{\hbar\Omega}{2}\left(\sigma_- e^{i(\omega_L t - k_L \hat{q})} + \sigma_+ e^{-i(\omega_L t - k_L \hat{q})}\right) \tag{17.4}$$

where $\hat{q}$ is the operator for the displacement of the ion from its equilibrium position in the trap, ν is the trap (secular) frequency, Ω is the Rabi frequency for the two level transition, ω_A is the atomic transition frequency, and ω_L, k_L are the laser frequency and wave number. The sigma matrices are defined in Sect. 10.1. There are three frequencies in the problem: ν, ω_A and ω_L. By carefully choosing relationships between these three frequencies various quantum interactions between electron and vibrational degrees of freedom can be driven. The key point is that the phase of the laser field as seen by the ion depends on the position of the ion. As the ion vibrates this phase is modulated at the trap frequency, which leads to sidebands in the absorption spectrum for the two level system.

The ion position operator may be written,

$$\hat{q} = \left(\frac{\hbar}{2m\nu}\right)^{1/2}(a + a^\dagger) \tag{17.5}$$

We now define the Lamb-Dicke parameter, η

$$\eta = k_L\left(\frac{\hbar}{2m\nu}\right)^{1/2} = 2\pi\Delta x_{rms}/\lambda_L \tag{17.6}$$

where the r.m.s position fluctuations in the oscillator ground state is Δx_{rms}. Then moving to an interaction picture via the unitary transformation

$$U_0(t) = \exp[-i\nu a^\dagger a t - i\omega_A \sigma_z t] \tag{17.7}$$

the interaction Hamiltonian can be written as

$$H_I(t) = \frac{\hbar\Omega}{2}\left(\sigma_- \exp[-i\eta(ae^{-i\nu t} + a^\dagger e^{i\nu t})]\exp[-i(\omega_A - \omega_L)t] + \text{h.c}\right) \tag{17.8}$$

The exponential of exponentials make this a complicated Hamiltonian system. However in most ion trap experiments the ion is confined to a spatial region that is significantly smaller than the wavelength of the exciting laser so that we may assume that the Lamb-Dicke parameter is small $\eta < 1$ (typically $\eta \approx 0.01 - 0.1$). Expanding the interaction to second order in the Lamb-Dicke parameter gives

$$\begin{aligned} H_I(t) = & \frac{\hbar\Omega}{2}[1 - \eta^2 a^\dagger a]\left(\sigma_- e^{-i\delta t} + \sigma_+ e^{i\delta t}\right) \\ & -i\,\frac{\hbar\Omega\eta}{2}\left(ae^{-i\nu t} + a^\dagger e^{i\nu t}\right)e^{-i\delta t}\sigma_- + i\,\frac{\hbar\Omega\eta}{2}\left(ae^{-i\nu t} + a^\dagger e^{i\nu t}\right)e^{i\delta t}\sigma_+ \\ & -\frac{\hbar\Omega\eta^2}{4}\left(a^2 e^{-2i\nu t} + (a^\dagger)^2 e^{2i\nu t}\right)\left(e^{-i\delta t}\sigma_- + e^{i\delta t}\sigma_+\right) \end{aligned}$$

where the detuning of the laser from the atomic frequency is $\delta = \omega - \omega_L$.

Tuning the frequencies so that δ is a positive or negative integer multiple of the trap frequency leads to resonant terms, and all time dependent terms are neglected. For carrier excitation, $\delta = 0$, the resonant terms are

$$H_c = \hbar\Omega(1 - \eta^2 a^\dagger a)\sigma_x \qquad \text{carrier excitation} \tag{17.9}$$

where $\sigma_x = (\sigma_- + \sigma_+)/2$. If we take $\delta = \nu$ so that the laser frequency is detuned below (to the red of) the carrier frequency by one unit of trap frequency, $\omega_L = \omega_A - \nu$, the resonant terms are

$$H_r = i\,\frac{\hbar\eta\Omega}{2}\left(a\sigma_+ - a^\dagger\sigma_-\right) \qquad \text{first red sideband excitation} \tag{17.10}$$

This is the Jaynes-Cummings Hamiltonian except that it involves the absorption of a trap *phonon* as well as one laser photon. If we instead choose $\delta = -\nu$ so that $\omega_L = \omega_A + \nu$, the laser is detuned one unit of vibrational frequency above the carrier (a blue detuning), the resonant interaction Hamiltonian is

$$H_b = i\,\frac{\hbar\eta\Omega}{2}\left(a^\dagger\sigma_+ - a\sigma_-\right) \qquad \text{first blue sideband excitation} \tag{17.11}$$

This corresponds to an excitation process in which one photon is absorbed from the laser and one trap phonon is *emited* . We can continue to define the second red sideband excitation $\delta = 2\nu$ and second blue sideband excitation $\delta = -2\nu$, and so

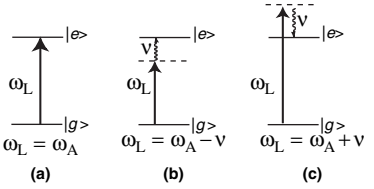

Fig. 17.2 Energy level diagram for (**a**) carrier (**b**) first red sideband and (**c**) first blue sideband excitation

on. In fig. 17.2 we give an energy level diagram that represents the carrier, red and blue sideband excitations.

An ion that is excited to $|e\rangle$ can spontaneously decay to the ground state, enabling another excitation. If we are tuned to the first red side band these cycles of excitation and emission remove one phonon per excitation cycle, thus cooling the vibrational degree of freedom. The external laser has coupled the vibrational motion to a very low temperature heat bath: the vacuum radiation field at frequency ω_A. For obvious reasons this is know as *side band cooling*. Needless to say this is only possible if we can spectroscopically resolve the red sideband. The width of each resonance is due to the spontaneous emission rate, γ, so we require that $\nu > \gamma$. The spectrum of resonance fluorescence for a single trapped ion follows from the methods given in Chap. 11. A detailed calculation in the low intenisity limit ($\Omega < \gamma$) for a traveling wave field, by Cirac et al. [6] shows that the spectrum of the motional sidebands exhibits the following features:

- The first red side band is centred on $\omega_L = \omega_A - \nu$ and the first blue sideband is centred on $\omega_L = \omega_A + \nu$ with linewidths determined by

$$\gamma_s = \eta^2 \left(\frac{\Omega}{2}\right)^2 [P(\nu+\delta) - P(\nu-\delta)] \tag{17.12}$$

  where $P(\delta) = \gamma/(\gamma^2 + \delta^2)$ and $\delta = \omega_L - \omega_A$ and γ is the spontaneous emission rate.
- The ratio of the peak height of the red sideband to the blue side band is $(\bar{n}+1)/\bar{n}$ where $\bar{n}$ is the steady state mean photon number of vibrational excitation.

Note that the heights of the peaks are different reflecting the fact that the red transition involves the absorption of a phonon while the blue involves the emission of a phonon.

In the Lamb-Dicke limit relaxation is dominated by spontaneous emission into the spectral peak at the carrier frequency ($\omega = \omega_A$) so that one unit of vibrational energy is removed on average per excitation cycle. We can understand this via a simple rate equation approach. In Exercise 17.1, we find that the rate of change of the average phonon number is given by

$$\frac{d\bar{n}}{dt} = -\gamma\left(\frac{\eta^2\Omega^2\bar{n}}{2\eta^2\Omega^2\bar{n} + \gamma^2}\right) \tag{17.13}$$

To be more realistic we also need to consider heating mechanisms, for example off-resonant excitation of the blue sideband [5], and the probability of populating the vibrational ground state in the steady state is less than unity. Despite the effects of heating, resolved sideband cooling care prepare an ion in the vibrational ground state with a probability greater than 99%, and was first achieved by the NIST group in Boulder [7]. Another source of heating that is difficult to control is due to fluctuating charge distributions on the trap electrodes. As these potentials change randomly in time, they produce a stochastic displacement of the centre of the trap. In Exercise 17.2 we consider this example in more detail.

We now turn to the problem of reading out the state of the ion. This is done by the technique of a cycling fluorescent transition which requires an additional auxiliary level, coupled by a strong probe laser to one or the other of the ground or excited states. We will consider the readout of the ground state (see Fig. 17.3). If the ion is in the ground state when the probe laser is turned on, fluorescent photons are scattered in all directions and can easily be detected. On the other hand if the ion is in the excited state, it is not resonant with the probe laser and no photons are scattered: the ion remains dark.

The interesting phenomenon of fluorescent shelving will now arise if a second weak laser induces incoherent transitions on $|g\rangle \leftrightarrow |e\rangle$. These transitions are incoherent as the strong coupling to the $|a\rangle$ state destroys coherence between the ground and excited states, see [8]. The fluorescent signal due to the strong probe laser switches on and off in the fashion of a random telegraph process. A typical signal is shown in 17.3. In so far as fluorescence indicates that the ion is in the ground state, the random switching of the fluorescence is a direct indicator of *quantum jumps* between the ground and excited states [3].

The quality of the readout can be reduced to a single number, called the efficiency, which is the conditional probability for a fluorescent photon to be detected *given* the ion is in the ground state. This is a function of the integration time of the fluorescent signal and the overall detection efficiency of the detection system.

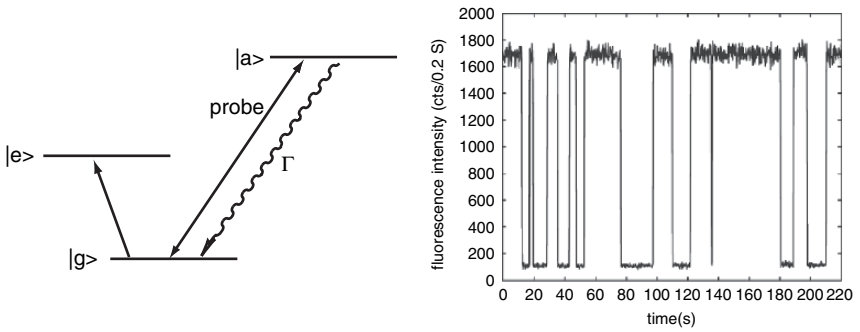

Fig. 17.3 Energy level diagram showing fluorescence readout of the ground atomic state. A strong probe laser drives a dipole allowed transition between the ground state $|g\rangle$ and an auxilary state $|a\rangle$ which decays back to the ground state at a rate Γ scattering many many photons. Also show is fluorescent signal on the probe transition when a weak laser couples the ground and excited state (reproduced, with permission, from Leibfried et al. [5]

The integration time should be at least of the order of the average time between photon emission events. In practice other sources of error must be considered,such as dark counts in the detector. Typically the minimum time to distinguish ground and excited states is of the order of 2 ms.

How efficient is the process of sideband cooling? We can only answer this if we have an independent way to determine the vibrational state of the ion at the end of a cooling phase. This may be done by coupling the vibrational motion to the internal state of the ion and then using the fluorescent readout technique described above. Suppose the electronic state of the ion can be coupled to its vibrational motion for a time T using either the first red and blue sideband transitions. If we write the probability for the atom to found in the excited state after time T as $P_e^R(T)$ and $P_e^B(T)$ for red and blue sideband excitation respectively it can be shown (see Exercise 17.3) that the mean phonon number $\bar{n}$ is given by $\bar{n}/(1+\bar{n}) = P_e^R(T)/P_e^B(T)$. Thus measurement of the ratio of excitation probability on the first red and blue sideband yields $\bar{n}$ directly.

17.3 Novel Quantum States

The ability to carefully control the coupling between internal electronic state of the ion and its vibrational motion in the trap enables us to carefully engineer novel quantum states of the vibrational degree of freedom. As an example we will here consider the preparation of a "cat state": a pure quantum state in which the two internal electronic states are correlated with different coherent states of the oscillator.

There are a number of ways to prepare the vibrational motion in a coherent state, $|\alpha\rangle$. The ion is first cooled to the vibrational ground state. A classical uniform driving force oscillating at the secular frequency, ν, can then be applied by changing the bias conditions on the trap electrode. Alternatively a non adiabatic displacement of the trap centre can be made again by changing the bias conditions. Finally a spatially varying Stark shift can be applied by using the moving standing wave that results from two laser beams with frequency difference $\Delta\omega = \nu$ to resonantly drive the motion of the ion in the trap. If the laser polarisation is carefully chosen this will result in a force that depends on the internal electronic state. From the point of view of the electronic and vibrational states, this is a two photon Raman process depicted in Fig. 17.4 that Stark shifts the excited state $|e\rangle$. We will refer to this choice of Raman pulses as the Raman displacement pulse. If we detune the Raman lasers by a frequency $\Delta\omega = \omega_{\mathrm{A}}$ we can drive a carrier transition that coherently superposes the ground and excited states. We will refer to this choice of Raman pulses as the carrier pulse.

The state-dependent displacement is described by the interaction picture Hamiltonian

$$H_d = \hbar\chi(t)(a + a^\dagger)|e\rangle\langle e| + \hbar\Omega(t)\sigma_x \tag{17.14}$$

the coupling constants χ and Ω are shown as time dependent as they can be turned on and off with the external Raman displacement pulse (χ) or the external carrier pulse (Ω).

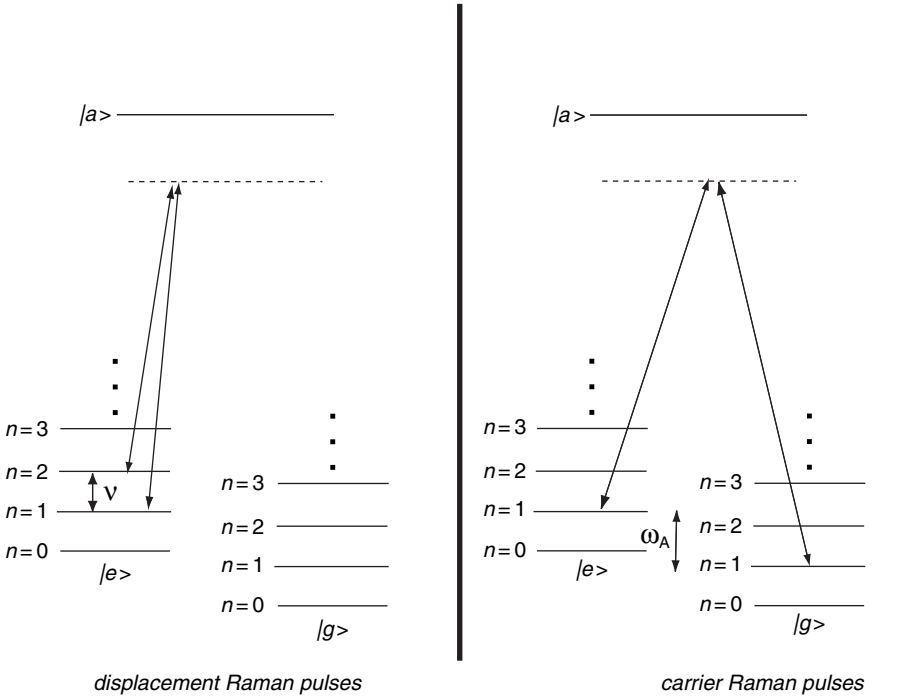

Fig. 17.4 A schematic indication of the optical transitions required to prepare a single ion in a linear superposition of displaced ground states (coherent states). On the left is the Raman pulse excitation scheme for applying a force to the ion conditional on it being prepared in the excited electronic state. On the right is the carrier pulse excitation scheme for producing coherent excitations of the internal electronic state leaving the vibrational motion unaffected. The vibrational frequency is ν while the atomic transition frequency is ω_a

Assume that initially the electronic system and vibrational motional are in the ground state, $|\psi(0)\rangle = |0\rangle \otimes |g\rangle$. In the first step, we apply a carrier pulse (so $\chi = 0$) for a time, T, such that $\omega T = \pi/2$. This gives the state transformation

$$|0\rangle \otimes |g\rangle \stackrel{\pi/2}{\Longrightarrow} |0\rangle \otimes \frac{1}{\sqrt{2}}(|g\rangle + |e\rangle) \tag{17.15}$$

In the second step we turn off the carrier pulse and turn on the displacement Raman pulse for a time τ. Only the $|e\rangle$ component sees the displacement, according to (17.14) so the state is transformed as

$$\frac{1}{\sqrt{2}}(|0\rangle \otimes |g\rangle + |0\rangle \otimes |e\rangle) \stackrel{\text{displace}}{\Longrightarrow} \frac{1}{\sqrt{2}}(|0\rangle \otimes |g\rangle + |\alpha\rangle \otimes |e\rangle) \tag{17.16}$$

In the third step we apply a $\pi = \Omega T$ carrier pulse that flips the electronic states and inserts a π phase shift

$$\frac{1}{\sqrt{2}}(|0\rangle \otimes |g\rangle + |\alpha\rangle \otimes |e\rangle) \stackrel{\pi}{\Longrightarrow} \frac{1}{\sqrt{2}}(|\alpha\rangle \otimes |g\rangle - |0\rangle \otimes |e\rangle) \tag{17.17}$$

In the fourth step we apply another state selective displacement with a relative phase ϕ,

$$\frac{1}{\sqrt{2}}(|\alpha\rangle \otimes |g\rangle - |0\rangle \otimes |e\rangle) \stackrel{\text{displace}}{\Longrightarrow} \frac{1}{\sqrt{2}}(|\alpha\rangle \otimes |g\rangle - |\alpha e^{i\phi}\rangle \otimes |e\rangle) \tag{17.18}$$

In the fifth and final step, we apply another $\pi/2$ pulse to give

$$\begin{aligned}\frac{1}{\sqrt{2}}(|\alpha\rangle \otimes |g\rangle - |\alpha e^{i\phi}\rangle \otimes |e\rangle) &\stackrel{\pi/2}{\Longrightarrow} \left(\frac{|\alpha\rangle - |\alpha e^{i\phi}\rangle}{2}\right) \otimes |g\rangle + \left(\frac{|\alpha\rangle + |\alpha e^{i\phi}\rangle}{2}\right) \otimes |e\rangle \\ &\equiv |\alpha_-\rangle \otimes |g\rangle + |\alpha_+\rangle \otimes |e\rangle \end{aligned} \tag{17.19}$$

If we now readout the state of the ion, the conditional states are highly non classical superpositions of two different coherent states of vibrational motion, $|\alpha_\pm\rangle$ known in quantum optics as *cat states*.

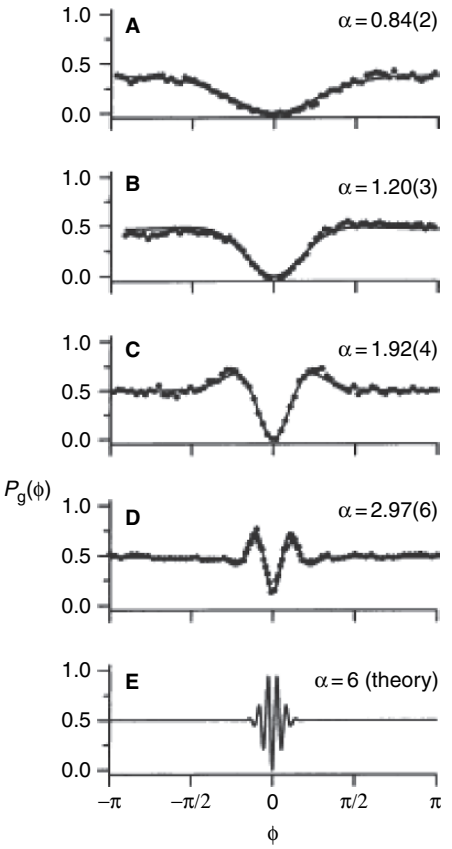

Fig. 17.5 The probability to find the ion in the ground state as a function of the phase of displacements for different choices of the magnitude of displacement. From Fig. 4 of Monroe et al., Science, **272**, 1135 (1996)

We thus have correlated different motional states with each of the electronic states. This kind of entangled state is reminiscent of Schrödinger's famous thought experiment in which two different metabolic (and thus macroscopic) states of a cat are correlated with a two level system in just this way. Indeed if we stopped after the second step the cat state analogy could be sustained with the identification $|\alpha\rangle \rightarrow |\text{alive}\rangle$ and $|0\rangle \rightarrow |\text{dead}\rangle$. However pursuing the analogy to the final state at the end of step 5 produces the rather disturbing prospect (for the cat at least) of correlating different superposition of metabolic states with the internal electronic states. It is for this reason that superpositions of coherent states are called cat states in quantum optics.

In the experiment of Monroe at al. [9], the presence of an entangled state of different coherent states was demonstrated by measuring the electronic state at the end of step 5. Repeated measurements enabled a sampling of the distribution $P_g(\phi)$, for different values of ϕ. This is given by

$$\begin{aligned} P_g(\phi) &= \langle \alpha_- | \alpha_- \rangle \\ &= \frac{1}{2}\left[1 - e^{-|\alpha|^2(1-\cos\phi)} \cos\left(|\alpha|^2 \sin\phi\right)\right] \end{aligned} \tag{17.20}$$

In Fig. 17.5 we reproduce the results from Monroe et al. [9] comparing the experiment with the theoretical prediction in Eq. 17.20. The agreement is remarkable.

17.4 Trapping Multiple Ions

In a linear ion trap such as depicted in Fig. 17.1, multiple ions may be trapped and cooled to the collective ground states of vibrational motion. Each ion has an equilibrium position, $\bar{x}_i$, corresponding to a minimum in the total potential comprising the trap plus Coulomb potential for each ion. These equilibrium points are analogous to the atomic ions at the lattice points of a crystal, however unlike a crystal they are not equally spaced. In terms of a natural length scale given by the Coulomb potential for each ion,

$$l = \left(\frac{Z^2 e^2}{4\pi\varepsilon_0 M \nu^2}\right)^{1/3}, \tag{17.21}$$

and a coordinate system in which $z = 0$ is in the middle of the trapped ions, *James* [10] has computed the equilibrium positions for different numbers of ions in a trap, see Fig. 17.6

If we expand the overall potential to second order in the small oscillations, $q_n(t)$ (in dimensionless units), around the equilibrium points we obtain a simple coupled oscillator Hamiltonian of the form,

$$H = \frac{1}{2M}\sum_{n=1}^{N} p_m^2 + \frac{M\nu^2}{2}\sum_{n,m=1}^{N} A_{nm} q_n q_m \tag{17.22}$$

N	Scaled equilibrium positions									
2					−0.62996		0.62996			
3				−1.0772		0		1.0772		
4			−1.4368		−0.45438		0.45438		1.4368	
5			−1.7429		−0.8221	0		0.8221		1.7429
6		−2.0123		−1.1361		−0.36992	0.36992		1.1361		2.0123
7		−2.2545		−1.4129		−0.68694	0	0.68694		1.4129		2.2545
8	−2.4758		−1.6621		−0.96701		−0.31802	0.31802		0.96701		1.6621		2.4758
9		−2.6803		−1.8897		−1.2195		−0.59958	0	0.59958		1.2195		1.8897		2.6803
10	−2.8708		−2.10003		−1.4504		−0.85378		−0.2821	0.2821		0.85378		1.4504		2.10003		2.8708

Fig. 17.6 The equilibrium positions for varying numbers of ions in the trap in units of the length scale given in 17.21. From Fig. 1 James et al. Appl. Phys. B, 66, 181, (1998)

where p_n is the canonical momentum to q_n. Explicit expressions for the coefficients A_{nm} are given in [10]. This Hamiltonian represents a linear array of N simple harmonic oscillators with quadratic coupling. We can now make a change of variable to normal-mode coordinates (sometimes called collective or global coordinates). The transformation is chosen to diagonalise the real symmetric $N \times N$ matrix with entries A_{nm}. The eigenvalue equation is

$$\sum_{n=1}^{N} A_{nm}\beta_n^{(p)} = \mu_p \beta_m^{(p)} \quad (p = 1, \ldots, N) \tag{17.23}$$

where the eigenvalues are $\mu_p > 0$ and the eigenvectors $\vec{\beta}^{(p)}$ are assumed to be numbered in order of increasing eigenvalue and are normalised so that

$$\sum_{p=1}^{N} \beta_n^{(p)} \beta_m^{(p)} = \delta_{nm}$$

$$\sum_{n=1}^{N} \beta_n^{(p)} \beta_n^{(q)} = \delta_{pq}$$

For example, when $N = 3$ the eigenvalues are $\mu_1 = 1, \mu_2 = 3, \mu_3 = 29/5$. The normal modes are then given in terms of the small oscillations as

$$Q_p(t) = \sum_{m=1}^{N} \beta_m^{(p)} q_m(t) \tag{17.24}$$

Note the number of normal modes is equal to the number of ions. Of course we can equally well write the *local coordinates* q_n as

$$q_m(t) = \sum_{p=1}^{N} \beta_m^{(p)} Q_p(t) \tag{17.25}$$

The first normal mode, Q_1 represents the centre of mass mode in which all the ions oscillate as if they were train wagons linked together. The second mode Q_2 represents a breathing mode in which each ion oscillates with an amplitude proportional to is displacement form the trap centre. In terms of the normal mode coordinates, Q_p and conjugate momenta P_p, the Hamiltonian is

$$H = \frac{1}{2M}\sum_{p=1}^{N} P_p^2 + \frac{M}{2}\sum_{p=1}^{N} \nu_p^2 Q_p^2 \tag{17.26}$$

where the frequencies of each of the normal modes is given by

$$\nu_p = \nu\sqrt{\mu_p} \tag{17.27}$$

This is the Hamiltonian of N independent simple harmonic oscillators. Thus we introduce raising and lowering operators for each normal mode as

$$Q_p = \sqrt{\frac{\hbar}{2M\nu_p}}(b_p + b_p^\dagger) \tag{17.28}$$

$$P_p = -\mathrm{i}\sqrt{\frac{\hbar M\nu_p}{2}}(b_p - b_p^\dagger) \tag{17.29}$$

with $[b_p, b_q^\dagger] = \delta_{pq}$.

Let us now assume that each ion in the trap can be addressed with a separate laser beam. For example in a linear ion trap for $^{40}Ca^+$ built in Innsbruck, the average spacing for 4 ions was greater than 5 μm, which is above the diffraction limit for the laser beams. This spacing is also sufficient for the fluorescence (at readout) of each ion to be separately imaged.

The interaction picture Hamiltonian describing how the ith ion is coupled to small oscillations around equilibrium is given by an obvious generalisation of Eq. 17.4

$$H_I^{(i)} = \hbar\frac{\Omega_i}{2}\left(\sigma_-^{(i)}\mathrm{e}^{-\mathrm{i}k_\mathrm{L}(q_i(t)}\mathrm{e}^{-\mathrm{i}(\omega_\mathrm{A}-\omega_\mathrm{L})t} + \mathrm{h.c}\right) \tag{17.30}$$

where we have taken the Rabi frequency for the ith ion to be Ω_i and $\sigma_\pm^{(i)}$ are the Pauli raising and lowering operators for the ith ion, while $q_i(t)$ are local coordinates of the ith ion. If we now again assume that the Lamb–Dicke parameter for each ion is small, the interaction between the electronic and vibrational degree of freedom is

$$H_I^{(i)} = -i\hbar\frac{k_\mathrm{L}\Omega_i}{2}\left(\sigma_-^{(i)}q_i(t)\mathrm{e}^{-\mathrm{i}(\omega_\mathrm{A}-\omega_\mathrm{L})t} - \mathrm{h.c}\right) \tag{17.31}$$

This may be written in terms of the global modes as

$$H_I^{(I)} = -i\hbar\frac{\eta\Omega_i}{2\sqrt{N}}\sum_{p=1}^{N} s_i^{(p)}\left(b_p\mathrm{e}^{-\mathrm{i}\nu_p t} + b_p^\dagger\mathrm{e}^{\mathrm{i}\nu_p t}\right)\mathrm{e}^{-\mathrm{i}(\omega_\mathrm{A}-\omega_\mathrm{L})t}\sigma_-^{(i)} - \mathrm{h.c} \tag{17.32}$$

where $s_p^{(i)} = \sqrt{N}\mu_p^{-1/4}\beta_i^{(p)}$.

We now assume that we can tune the external laser to address only a single global vibrational mode (a particular normal mode), say the centre of mass mode at frequency, $\mu_1 = \nu$ and $s_i^{(1)} = 1$ with $\omega_\mathrm{A} - \omega_\mathrm{L} = \nu$. Then we can ignore all the other modes and approximate the Hamiltonian as

$$H_I^{(i)} = -i\hbar\frac{\eta\Omega_i}{2\sqrt{N}}\left(\sigma_+^{(i)}b_1 + \sigma_-^{(i)}b_1^\dagger\right) \tag{17.33}$$

This is the Cirac–Zoller Hamiltonian [1] and was used by these authors in a scheme for quantum computing using trapped ions (see below). If there are many ions in the trap this may not be a good approximation. In that case there are many normal modes and it is difficult to resolve individual normal mode frequencies as they become very closely spaced. To some extent this may be mitigated by cooling all the normal modes to their ground states. Further discussion of the validity of this approximation may be found in [10] and also [11].

There is an interesting interpretation of the Hamiltonian for local modes, (17.31). Define

$$\sigma_1^{(i)}(t) = \sigma_- \mathrm{e}^{-\mathrm{i}\Delta t} + \sigma_+ \mathrm{e}^{\mathrm{i}\Delta t} \tag{17.34}$$

with $\Delta = \omega_\mathrm{A} - \omega_\mathrm{L}$. Now define a quantum field $\hat{\psi}(x,t) = (2M\nu/\hbar)^{1/2}q_i(t)$ by replacing the discrete index, i, with a position variable $x = \mathrm{i}d_i$ where d_i is the position of the ith ion form the centre of the trap. This field is a scalar field operator describing the small oscillations of the ion at x from equilibrium. The interaction Hamiltonian then takes the form

$$H_I = \hbar\chi\,\hat{\psi}(x,t)\sigma_1(x,t) \tag{17.35}$$

which is in the form of local field dipole detector interaction Hamiltonian, with $\chi = \eta\Omega/2$.

17.5 Ion Trap Quantum Information Processing

In 1995 Cirac and Zoller [1] proposed the first scheme for implementing quantum logic gates for trapped ions. In a quantum computer information is stored in the states of a collection of two level systems, generically referred to as qubits. In the Cirac–Zoller (CZ) scheme, the qubits are the two-level electronic states of the trapped ions. Arbitrary transformations of the state of a single qubit are easily implemented by external laser fields. For universal computation we also need to have access to two qubit interactions. However the electronic states of different ions do not interact. CZ proposed to overcome this by using the collective vibrational mode of the ions to implement a virtual interaction between the qubits.

We will discuss a way to implement a particular two qubit interaction, known as a controlled NOT (CNOT) gate which is a universal two-qubit gate. If we denote the two states of a qubit as $|x\rangle, x = 0,1$, the CNOT gate is defined by the unitary transformation

$$U_{CN}|x\rangle \otimes |y\rangle = |x\rangle \otimes |x \oplus y\rangle \tag{17.36}$$

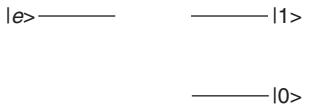

Fig. 17.7 The electronic level scheme for each ion in the CNOT gate scheme of Cirac and Zoller

where $x \oplus y$ is addition modulo two. In words, the state of the second qubit, called the target, is flipped if and only if the state of the first qubit, the control, is $|1\rangle$. In all cases the state of the control qubit is unchanged.

In the CZ scheme each ion has a set of internal electronic levels, $|\mathrm{o}\rangle, |\mathrm{1}\rangle$ and $|e\rangle$, depicted in Fig. 17.7. The mapping between physical electronic states and logical states is $|\mathrm{o}\rangle \leftrightarrow |0\rangle,\ |\mathrm{1}\rangle \leftrightarrow |1\rangle$. Note that in addition to the qubit states, there is an additional auxiliary state, $|e\rangle$ which helps implement the degree of control required. We suppose that is possible to direct a laser onto a particular ion inducing electronic transitions in that ion alone. This can couple the qubit state of the ion to its vibrational degree of freedom. In the Lamb–Dicke limit and for carefully chosen detunings, it is possible to couple a single qubit state to a chosen collective state of vibrational motion of all the trapped ions. In the CZ scheme the collective vibrational modes are all prepared in the ground state by a prior sideband cooling step.

Let us suppose the laser is directed towards the nth ion and tuned to the first red sideband of the collective centre of mass mode described by raising and lowering operators, $a^\dagger, a$. The Hamiltonian for this is

$$H = \hbar \frac{\eta\Omega}{2\sqrt{N}} (a|\mathrm{1}\rangle_n\langle \mathrm{o}|\mathrm{e}^{-\mathrm{i}\phi} + a^\dagger|\mathrm{o}\rangle_n\langle \mathrm{1}|\mathrm{e}^{\mathrm{i}\phi}) \tag{17.37}$$

If this laser is on for a time T such that $\eta\Omega T\sqrt{N} = k\pi$ (a $k\pi$-pulse), the unitary operator,

$$U^{k,n}_{\mathrm{o1}}(\phi) = \exp\left[-\mathrm{i}\frac{\pi}{2}(a|\mathrm{1}\rangle_n\langle \mathrm{o}|\mathrm{e}^{-\mathrm{i}\phi} + a^\dagger|\mathrm{o}\rangle_n\langle \mathrm{1}|\mathrm{e}^{-\mathrm{i}\phi})\right] \tag{17.38}$$

is implemented. This unitary interaction couples the electronic states to the vibrational phonon number states $|0\rangle, |1\rangle$;

$$U^{k,n}_{\mathrm{o1}}(\phi)|\mathrm{o}\rangle_n|1\rangle = \cos(k\pi/2)|\mathrm{o}\rangle_n|1\rangle - \mathrm{i}\mathrm{e}^{\mathrm{i}\phi}\sin(k\pi/2)|\mathrm{1}\rangle_n|0\rangle \tag{17.39}$$

$$U^{k,n}_{\mathrm{o1}}(\phi)|\mathrm{1}\rangle_n|0\rangle = \cos(k\pi/2)|\mathrm{1}\rangle_n|0\rangle - \mathrm{i}\mathrm{e}^{-\mathrm{i}\phi}\sin(k\pi/2)|\mathrm{o}\rangle_n|1\rangle \tag{17.40}$$

We will also need to implement $k\pi$ pulse between the ground state $|\mathrm{o}\rangle$ and the auxiliary excited state $|e\rangle$. This implements the unitary transformation

$$U^{k,n}_{\mathrm{o}e}(\phi) = \exp\left[-\mathrm{i}\frac{\pi}{2}(a|e\rangle_n\langle \mathrm{o}|\mathrm{e}^{-\mathrm{i}\phi} + a^\dagger|\mathrm{o}\rangle_n\langle e|\mathrm{e}^{-\mathrm{i}\phi})\right] \tag{17.41}$$

and can be done by changing the polarisation of the exciting laser.

We now consider a three pulse sequence: on the mth ion implement $U^{1,m}_{\mathrm{o1}}(0)$, then on the nth ion a 2π pulse between the ground state and the auxillary excited state, $U^{2,n}_{\mathrm{o}e}(0)$, finally, again on the m'th ion, $U^{1,m}_{\mathrm{o1}}(0)$. The three pulse sequence thus implements the product unitary, $U^{m,n} = U^{1,m}_{\mathrm{o1}}(0)U^{2,n}_{\mathrm{o}e}(0)U^{1,m}_{\mathrm{o1}}(0)$. Acting on each of

the four possible two qubit states of the ions we find that all states remain unchanged except when both ions are initially excited;

$$|1\rangle_m|1\rangle_n \rightarrow -|1\rangle_m|1\rangle_n \tag{17.42}$$

This is a two qubit gate known as the CSIGN gate. To use this to implement a CNOT gate we now choose one of the ions to be the control qubit, say mth ion, and first use a laser pulse to put it into a superposition of the logical states, $|0\rangle_m + |1\rangle_m$. This can be done by tuning the laser to the carrier frequency so that it is resonant with the $|0\rangle_m \leftrightarrow |1\rangle_m$ transition, adjusting the phase and pulse area to implement the unitary

$$V_m = \exp\left[-\frac{\pi}{4}(|1\rangle_m\langle 0| - \text{h.c.})\right] \tag{17.43}$$

After we implement the V single qubit unitary on the mth ion we implement a CSIGN between the mth ion and the nth ion, target ion. Finally we again act with a V pulse on the mth ion. The net effect is to implement a CNOT gate between the mth ion as the control on the nth ion as the target. Clearly the ions do not need to be adjacent. Furthermore we can implement a number of CNOT gates between different pairs in parallel so long as we can individually resolve the ions with the control lasers. The Cirac–Zoller scheme was first implemented by the Innsbruck group led by Blatt in 2003 [12]. They used two $^{40}Ca^{+}$ ions held in a linear trap and individually addressed by focussed laser beams.

Other schemes have been proposed for implementing quantum gates in ion traps. *Sørenson* and *Mølmer* [13] developed a scheme which mitigates to some extent the deleterious effects of noise entering via the vibrational degree of freedom (e.g. patch potential heating) and implemented by the Wineland group in NIST [14]. A related scheme [15] uses far off-resonance optical dipole forces to implement a geometric phase gate, also first implemented by the NIST group [16]. The basic idea of a geometric phase gate is to use a sequence of laser pulse sequences, applied to two ions, that move the vibrational degree of freedom of the ion through a loop in phase space that depends on the internal states of the two ions. A simple, though impractical, way to achieve this is to use phase space displacements that move around a rectangle in phase space, starting at the origin, in a direction that depends on the internal state of the ion. For example, the unitary operators

$$U_j(\kappa_x) = \mathrm{e}^{-\mathrm{i}\kappa_x \hat{p}\sigma_{z,n}/\hbar} \tag{17.44}$$

$$U_j(\kappa_p) = \mathrm{e}^{-\mathrm{i}\kappa_p \hat{x}\sigma_{z,n}/\hbar} \tag{17.45}$$

give conditional displacements of the vibrational degree of freedom along the x-axis for the jth ion in the case of $U_j(\kappa_x)$ and along the p-axis in the case of $U_j(\kappa_p)$. If we use the commutation relation $[\hat{x}, \hat{p}] = i\hbar$ we can show that the following

$$U_k(\kappa_p)U_j(-\kappa_x)U_k(-\kappa_p)U_j(\kappa_x) = e^{i\kappa_x\kappa_p\sigma_{z,j}\sigma_{z,k}} \tag{17.46}$$

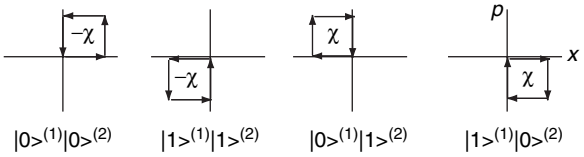

Fig. 17.8 The conditional phase space displacements of the vibrational degrees of freedom of two ions. Four cases are shown corresponding to the four distinct states of two qubits. The path followed is different for each case but the enclosed area is the same

This is an Ising-like two qubit unitary interaction between the j,kth qubits. Note that there is no dependance on the vibrational degree of freedom at all. Inspection of the various phase space orbits, see Fig. 17.8 indicates why this is called a geometric phase gate. The effective conditional phase between the two qubits is proportional to the area of the rectangle, $\chi = \kappa_x \kappa_p$ and the sign is given by the sense of rotation. It is clear that the actual shape of the closed orbit in phase space does not matter: only the area and sense of rotation matter. In an experiment the phase space rotations are done by a time varying driving fields, with both amplitude and phase modulation (see Exercise 17.3). The idea of conditional phase space displacements opens up a path to fast quantum gates for two ions [17].

Exercises

17.1 A laser is tuned to the first read sideband transition for a single two level transition, $|g\rangle \leftrightarrow |e\rangle$, with a spontaneous emission rate of γ. Ignoring all but the spontaneous emission decay channel, the master equation (in the interaction picture) describing this system is

$$\frac{\mathrm{d}\rho}{\mathrm{d}t} = \frac{\eta\Omega}{2}[a\sigma_+ - a^\dagger\sigma_-, \rho] + \gamma\mathscr{D}[\sigma_-]\rho \tag{17.47}$$

where η is the Lamb–Dicke parameter, Ω is the Rabi frequency for the transition and $a, a^\dagger$ are the lowering and raising operators for the vibrational motion of the ion in the trap. Obtain equations of motion for $\bar{n} = \langle a^\dagger a\rangle$, $\langle a\rangle$, $\langle\sigma_\pm\rangle$, $\langle\sigma_z\rangle$ by factorising all higher order moments in the equations of motion. Assuming that the spontaneous emission rate is large enough so that the average polarisation $\langle\sigma_\pm\rangle$ is stationary and the vibrational motion is slaved to the atomic motion, show that the rate of change of $\bar{n}$ is given by (17.13).

17.2 A simple mode for the heating of a trapped ion due to fluctuation potentials may be given in terms of the Hamiltonian

$$H(t) = \hbar\nu a^\dagger a + \hbar\varepsilon(t)(a + a^\dagger) \tag{17.48}$$

where $\varepsilon(t)$ is fluctuating force term with the following classical moments

$$\bar{\varepsilon} = \mathscr{E}(\varepsilon(t)) = 0$$
$$G(\tau) = \mathscr{E}(\varepsilon(t)\varepsilon(t+\tau)) = \frac{D}{2\gamma}\mathrm{e}^{-\gamma|\tau|}$$

Show that the heating rate is given by

$$\frac{\mathrm{d}\langle a^{\dagger}a\rangle}{\mathrm{d}t} = \frac{\pi}{2}S(\nu) \tag{17.49}$$

where the noise power spectrum for the fluctuating force is defined by

$$S(\omega) = \frac{1}{2\pi}\int_{-\infty}^{\infty}\mathrm{e}^{-\mathrm{i}\omega t}G(\tau) \tag{17.50}$$

17.3 Show that if a harmonic oscillator in its ground state is subjected to a sequence of displacements in phase space that form a closed loop, the state is returned to the ground state up to an overall phase proportional to the area of the loop.

References

1. J.I. Cirac, P. Zoller: Phys. Rev. Letts. **74**, 4091 (1995)
2. H.G. Dehmelt: Bull. Am. Phys. Soc. **20**, 60 (1975)
3. J.C. Bergquist, R.G. Hulet, W.M. Itano, D.J. Wineland: Phys. Rev. Lett. **57**, 1699 (1986): W. Nagourney, J. Sandberg, H.G. Dehmelt: Phys. Rev. Lett. **56**, 2797 (1986); T. Sauter, W. Neuhauser, R. Blatt, P. E. Toschek: Phys. Rev. Lett. **57**, 1696 (1986)
4. Ch. Roos, Th. Zeiger, H. Rohde, H.C. Nägerl, J. Eschner, D. Leibfried. F. Schmidt-kaler, R. Blatt, Phys. Rev. Letts., **83**, 4713 (1999)
5. D. Leibfried, R. Blatt, C. Monroe, D. Wineland: Rev. Mod. Phys. **75**, 281 (2003)
6. J.I. Cirac, R. Blatt, P. Zoller, W.D. Philips: Phys. Rev. A **46**, 2668 (1992)
7. C. Monroe, D.M. Meekhof, B.E. King, S.R. Jefferts, W.M. Itano, D.J. Wineland, P.L. Gould: Phys. Rev. Lett. **75**, 4011 (1995)
8. M.J. Gagen, G.J. Milburn: Phys. Rev. A **45**, 5228 (1992)
9. C. Monroe, D.M. Meekhof, B.E. King, D.J. Wineland: Science, **272**, 1131 (1996)
10. D.F.V. James: Appl. Phys. B **66**, 181, (1998)
11. D.J. Wineland, C. Monroe, W.M. Itano, D. Liebfried, B.E. King, D.M. Meekhof: J. Res. Natl. Stand. Technol. **103**, 259 (1998)
12. F. Schmidt-Kaler, H. Häffner, M. Riebe, S. Gulde, G.P.T. Lancaster, T. Deuschle, C. Becher, C.F. Roos, J. Eschner, R. Blatt: Nature, **422**, 408, (2003)
13. A. Sørensen, K. Mølmer: Phys. Rev. A **62**, 022311 (2000)
14. C.A. Sackett, D. Kielpinski, B.E. King, C. Langer, V. Meyer, C.J. Myatt, M. Rowe, Q.A. Turchette, W.M. Itano, D.J. Wineland, C. Monroe: Nature, **404**, 256 (2000)
15. G.J. Milburn, S. Schneider, D.F.V. James: Fortschritte der Physik, **48**, 801 (2000)
16. D. Leibfried, B. De MArco, V. Meyer, D. Lucas, M. Barrett, J. Britton, W.M. Itano, B. Jelenkovic, C. Langer, T. Rosenband, D.J. Wineland: Nature, **422**, 412 (2003)
17. J.J. Garcia-Ripoll, P. Zoller, J.I. Cirac: Phys. Rev. Lett. **91**, 157901 (2004); L.-M. Duan: Phys. Rev. Lett. **93**, 100502 (2004)